International Core Journal of Engineering Volume 12 Issue 4, 2026
ISSN: 2414-1895 DOI: 10.6919/ICJE.202604_12(4).0023

A Spiral-Driven In-Pipe Detection Robot with RGB-D Recognition and Quantification Algorithm for Thermal Bulge Inspection

Siyu Wang, Jiayi Hao, Guijing Zhang, Ruxin Zhang, Ruihan Cheng*

North China University of Science and Technology, Tangshan 063210, China

*Corresponding author: 18714689@qq.com

Abstract

To address the limitations of conventional pipeline hot-spot detection methods-such as low efficiency, poor accuracy, and high costs-this paper proposes an autonomous mobile pipeline inspection robot system based on the Convolutional Block Attention Module (CBAM). The system integrates a stereo camera, an inertial measurement unit (IMU), and brushless motors, and employs an improved wheeled drive mechanism combined with a helical transmission structure to achieve autonomous navigation inside pipelines. By developing an RGB-D fusion-based image recognition algorithm and leveraging disparity calculation principles, the system accurately quantifies the proportion of hot spots relative to the total pipeline length, thereby evaluating their impact on subsequent dismantling operations. Experimental results demonstrate that the proposed system achieves a hot-spot detection accuracy of 96.7% and a localization error of less than 3 cm, significantly enhancing both the automation level and precision of pipeline inspection. This work provides an advanced technical solution to longstanding challenges in pipeline maintenance.

Keywords

Pipeline Inspection Robot; Hot-Spot Detection; CBAM Attention Mechanism; RGB-D Fusion; Autonomous Navigation.

1. Introduction

Type III polypropylene (PPR) pipes have become the dominant material in modern building water supply and drainage systems due to their excellent corrosion resistance, long service life, and cost-effectiveness. Currently, the market penetration of PPR pipes in this sector exceeds 90%, with annual consumption surpassing two million metric tons. The widespread adoption of PPR piping is largely attributed to its primary joining method-hot-melt fusion-which offers both reliability and ease of installation. However, this critical process is prone to a common yet inadequately addressed defect known as a “hot spot” . A hot spot refers to an internal protrusion formed at the joint when excess molten material accumulates due to overheating or misalignment during the fusion process. This defect reduces the effective inner diameter of the pipe, thereby restricting water flow, increasing localized pressure drop, and potentially leading to system failure over time.

Despite the significant impact of thermal nodules on the long-term performance of PPR piping systems, current acceptance protocols exhibit critical limitations. Existing standards rely almost exclusively on pressure testing to verify joint integrity, completely omitting any assessment of cross-sectional area reduction caused by thermal nodules. The absence of effective in-situ inspection methods renders this defect highly concealed. Consequently, a noticeable decline in water flow is often the first observable indicator of the problem-by which time remediation typically requires destructive cutting and extensive, system-wide pipe replacement. Such reactive maintenance incurs

ISSN: 2414-1895 DOI: 10.6919/ICJE.202604_12(4).0023

substantial economic costs and causes severe operational disruption. For instance, data from Beijing between 2019 and 2024 reveal a steady year-on-year increase in both the total length of pipes replaced and the associated expenses attributable to flow obstruction caused by thermal nodules.

To address the critical technological gap in the detection and quantification of thermal nodules, this study aims to develop a novel autonomous pipeline inspection robot. The primary objective is to establish an integrated system capable of non-destructive detection, precise quantification, and spatial localization of thermal nodules within PPR pipes. The proposed robot incorporates several advanced technologies: a wall-pressure-adaptive helical-drive mechanism designed to enhance traversability through complex piping networks; an RGB-D image fusion algorithm enhanced with the Convolutional Block Attention Module (CBAM) to improve the robustness of defect recognition; and an IMU-based navigation module enabling accurate spatial registration of detected anomalies.

The successful development of this system will yield three significant outcomes. First, it will enable high-precision three-dimensional detection and volumetric assessment of thermal nodules, transforming the current qualitative inspection approach into a data-driven, quantitative evaluation framework. Second, by providing accurate spatial coordinates of defects, the robot will facilitate targeted repairs, thereby minimizing unnecessary pipe removal and reconstruction. Ultimately, this technology will serve as a critical enabler for proactive pipeline health management, substantially reducing the enormous costs associated with large-scale remediation, enhancing the overall quality of pipeline installations, and ensuring the long-term safety and reliability of building fluid transport systems.

2. Research background and theoretical basis

2.1 Evolution and Limitations of Pipeline Non-Destructive Testing Technologies

Conventional non-destructive testing (NDT) methods for pipelines include manual visual inspection, borescope examination, and manual gauge-based measurements. Manual visual inspection is restricted to accessible pipe ends and cannot navigate long or bent pipeline segments. Borescopes suffer from limited field of view and often produce poor image quality in the dark, reflective interior environments of pipes [1]. Moreover, these approaches are purely qualitative-they cannot quantify the volume or cross-sectional reduction caused by internal protrusions such as thermal nodules. Similarly, manual measurements using calipers or plug gauges are only feasible at pipe terminations and are inapplicable to already-installed joints embedded within building structures.

To overcome the limitations of manual inspection methods, various pipeline inspection robots have been developed both domestically and internationally. Based on their locomotion mechanisms, these robots can be classified into wheeled, tracked, inchworm-type (peristaltic), helical-drive, and soft-bodied designs [2]. Wheeled robots offer high speed and good controllability but often struggle with wall adhesion in vertical pipes and maneuverability through bends [3]. Tracked robots provide greater traction; however, their bulky structure makes them unsuitable for small-diameter pipelines-such as typical PPR pipes, which range from 20 to 50 mm in diameter. Inchworm-type and origami-inspired soft robots demonstrate adaptability in pipelines with varying diameters, yet they suffer from limited payload capacity and slow inspection speeds [4].

2.2 Bottlenecks of Existing Technologies in Non-Metallic PPR Pipelines

Despite significant advances in robotic inspection systems for pipeline defect detection in recent years, current technologies still exhibit critical limitations when applied to non-metallic PPR pipes-commonly used in building water supply systems. Specifically, the following three challenges remain inadequately addressed:

Poor adaptability to complex pipeline geometries: Many robotic platforms cannot reliably traverse common architectural plumbing features such as 90° elbows, T-junctions, or vertical risers. The small internal diameter of PPR pipes (typically 20–50 mm) further restricts the deployment of bulkier mechanical designs.

ISSN: 2414-1895 DOI: 10.6919/ICJE.202604_12(4).0023

Lack of accurate in-pipe localization capability: Unlike metallic pipelines, which support electromagnetic sensing methods such as magnetic or eddy-current sensors, non-metallic PPR pipes are incompatible with such techniques. Moreover, GPS signals are unavailable inside building-embedded pipelines. Consequently, external positioning is infeasible, and robots must rely solely on onboard dead reckoning for navigation.

Inability to perform 3D spatial annotation of defects: Even when a defect is visually detected via onboard cameras, accurately mapping its location along both the axial (lengthwise) and circumferential directions of the pipe remains challenging without multi-sensor fusion. Most existing systems merely record video footage, requiring operators to manually estimate defect positions-a process that is subjective and error-prone.

Table 1. Comparison of Limitations in Defect Detection Technologies for Non-Metallic Pipelines

Comparison Dimension	Traditional Inspection Methods	Existing Robotic Inspection Systems	Key Limitations
Adaptability to Complex Geometries	Relies on manual operation; unable to access 90° elbows, T-junctions, or vertical risers; practically infeasible in small-diameter pipes (≤50 mm)	Most robots feature rigid structures and large turning radii, limiting navigation through tight bends and complex junctions in small-diameter pipes	Both approaches struggle to cover the typical topology of building water supply networks, especially dense and spatially constrained PPR piping systems
In-Pipe Localization Capability	No localization functionality; defect positions estimated subjectively based on operator experience	Lacks reliable localization methods suitable for non-metallic pipes; dead reckoning suffers from error accumulation	PPR material is incompatible with electromagnetic or GPS-based positioning, making precise spatial recall of defects unattainable
3D Spatial Annotation of Defects	Provides only 2D video/images; defect locations require manual inference; no axial or circumferential coordinates	Most systems do not integrate multi-sensor fusion (e.g., IMU, odometry, visual SLAM), hindering accurate spatial mapping	Defect records lack quantifiable and reproducible spatial information, compromising subsequent repair planning and condition assessment

2.3 Theoretical Foundations of Visual Perception and Inertial Navigation

Depth vision can acquire three-dimensional geometric information of a scene. Stereo vision is one of the most common depth sensing techniques, utilizing two calibrated cameras to compute a disparity map. The disparity of each pixel is inversely proportional to the distance from the camera to that point [5]. By combining RGB images with depth maps, an RGB-D representation is formed. This fusion is particularly advantageous for defect detection in pipeline environments, where textures are sparse or lighting conditions are uneven. Even if RGB signals are affected by reflections or darkness, the depth channel can accurately capture the shape and protrusion height of thermal nodules.

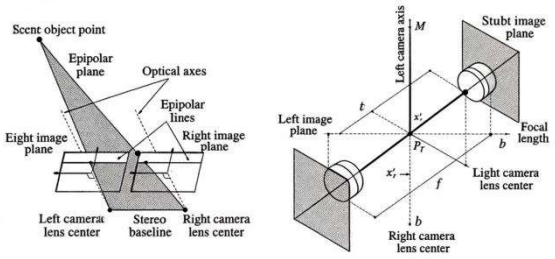

Figure 1. Geometric model of disparity and depth computation in stereo vision.

ISSN: 2414-1895 DOI: 10.6919/ICJE.202604_12(4).0023

Complementing the aforementioned vision-based depth perception, inertial measurement units (IMUs) typically consist of a triaxial accelerometer, a gyroscope, and sometimes a magnetometer. By integrating angular velocity over time, the IMU can estimate orientation. Furthermore, by double-integrating acceleration data after gravity compensation, it can estimate displacement relative to the starting point-a process known as dead reckoning [6]. The primary drawback of pure inertial navigation is cumulative drift caused by sensor noise and bias instability. Nevertheless, in enclosed, GPS-denied environments such as PPR pipelines, IMU-based dead reckoning remains the only viable approach for relative localization. This drift can be mitigated through complementary filtering or sensor fusion with visual odometry.

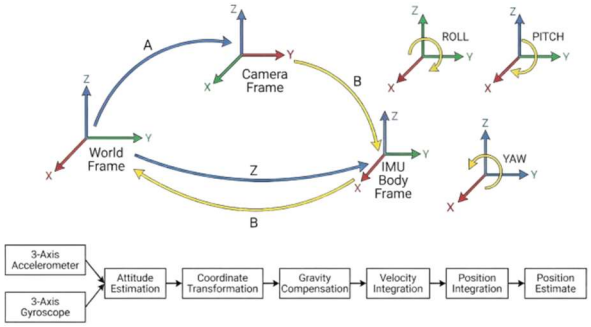

Figure 2. Dead reckoning based on IMU.

2.4 Theoretical Feasibility of Technical Integration

This project establishes an organically integrated inspection architecture by synergistically combining RGB-D visual perception, inertial navigation, and helical-drive locomotion. The stereo camera and IMU are rigidly mounted and spatially aligned through high-precision time synchronization and coordinate transformation. A cross-platform interactive interface, developed using PyQt5, provides real-time visualization of fused RGB-D imagery and thermal nodule localization trajectories on the front end. On the back end, image processing and inertial computation are executed on a Raspberry Pi 4B embedded platform; its multi-core CPU architecture efficiently supports the real-time operation of the CBAM attention mechanism and complementary filtering algorithms. Furthermore, data-level fusion between the IMU and visual odometry is achieved via an Extended Kalman Filter (EKF), enabling stable localization in GPS-denied, enclosed pipeline environments. Existing studies confirm that multi-sensor fusion significantly enhances both localization accuracy and defect detection performance in pipeline inspection robots [7][8].

This integrated architecture leverages the high-resolution capability of vision sensors for defect texture recognition while mitigating the risk of visual failure in dark or textureless conditions through inertial navigation. Simultaneously, the helical-drive mechanism provides a stable and controllable motion platform for sensor data acquisition. Together, these three technologies form a closed-loop workflow across data collection, feature fusion, and spatial annotation-thereby demonstrating the theoretical feasibility of multi-modal technical integration for non-destructive thermal nodule inspection inside pipelines.

3. System requirement analysis

3.1 Educational Scenario Requirements

The detection of thermal beads formed during the hot-melt connection of PPR pipes presents multiple challenges in engineering practice. Located inside the pipes, thermal beads are not directly observable from the exterior. Traditional detection methods can only locate thermal beads through destructive pipe cutting after a significant drop in water flow, resulting in severe resource waste and economic losses. The current acceptance system only conducts pressure tests for pipe tightness and does not incorporate the reduction in pipe cross-sectional area into the quality evaluation system. As a result,

ISSN: 2414-1895 DOI: 10.6919/ICJE.202604_12(4).0023

the volume, proportion, and impact of thermal beads on flow capacity cannot be quantified, and more than 70% of construction contractors judge the severity of thermal beads solely based on experience. In addition, PPR pipes are mostly non-metallic, making metal detection or GPS positioning inapplicable. The interior of the pipes is dark and narrow with elbows and tees, which makes it difficult to determine the robot's position, and detected thermal beads cannot be correlated with the actual spatial position of the pipes. In summary, there is an urgent need for an intelligent detection system capable of non-destructively entering pipes, automatically identifying and quantifying thermal beads, and providing accurate spatial positioning.

3.2 Requirements for Multimodal Visual Inspection

The interior of pipelines is extremely poorly lit with uneven illumination distribution, resulting in severe loss of texture information in ordinary RGB images. A single RGB camera struggles to capture the boundary features of thermal beads, especially when the color of thermal beads is similar to that of the pipe wall, which significantly increases detection difficulty. Therefore, the system needs to integrate depth images to obtain three-dimensional geometric features, requiring binocular cameras to stably output depth data even under low illumination.RGB images and depth maps are acquired by different sensors, leading to deviations in acquisition time and spatial coordinate systems. The system must complete spatiotemporal synchronization of the two modal data within milliseconds, ensuring that the color and depth information corresponding to the same pixel position belong to the same physical point inside the pipeline. This demands hardware with a high-precision time synchronization mechanism and software to complete internal parameter calibration and stereo rectification of the binocular cameras.Thermal beads present diverse morphologies, with irregular boundaries often caused by the flow of molten material, and no obvious color or texture mutation between thermal beads and normal pipe walls. Traditional object detection algorithms are prone to missed or false detections. The system needs to introduce an attention mechanism to enable the model to focus on geometric mutation areas provided by depth maps, compensating for the lack of boundary information in RGB images.The impact of thermal beads on pipeline flow capacity is determined by their volume ratio. The system needs to back-project depth pixels corresponding to segmentation masks to generate dense point clouds and reconstruct a closed 3D model. Engineering requirements stipulate that the relative volume error shall be controlled within 10% to support reliable determination of graded alarm thresholds.

3.3 Requirements for Inertial Navigation and Spatial Positioning

No external positioning beacons such as GPS, Wi-Fi or UWB can be deployed in non-metallic pipelines. The robot can only estimate its relative position using onboard sensors. The inertial measurement unit (IMU) is the only feasible solution for continuous positioning, yet low-cost IMU sensors suffer from severe zero-bias drift and cumulative errors.Integration of the gyroscope in the IMU causes attitude angles to drift over time, while relying solely on accelerometers and magnetometers is vulnerable to interference from pipeline vibration and motion. The system shall adopt complementary filtering or extended Kalman filtering (EKF) algorithms to fuse nine-axis data for stable attitude output, with a requirement that attitude angle drift does not exceed 5° per meter of travel distance.Thermal beads detected by the binocular camera are represented in the camera coordinate system, whereas the path information provided by the IMU is in the navigation coordinate system. The system shall establish the transformation relationship between the two coordinate systems through rigid fixation and precise extrinsic parameter calibration, and finally map the spatial coordinates of thermal beads to the global pipeline trajectory to assist workers in locating and cutting. For engineering applications, the error between the marked position of thermal beads and the actual position is required to be within 15 cm.

3.4 Requirements for Robot Driving Structure and Motion Control

The target pipeline diameter ranges from DN30 to DN50 with an inner diameter of 30–50 mm, and the overall dimensions of the robot shall be adapted to this range. Traditional wheeled driving

ISSN: 2414-1895 DOI: 10.6919/ICJE.202604_12(4).0023

structures have a large turning radius and difficulty passing through 90° elbows and tees. Therefore, the system shall adopt a screw-driven, wall-pressure-adaptive driving structure. The inclined wheel sets generate a helical motion trajectory to reduce sensitivity to bend curvature. The robot is required to stably pass through elbows with a curvature radius of no less than 1.5 times the pipe diameter.In building water supply and drainage systems, pipelines include vertical rising sections. The robot must overcome its own gravity to achieve vertical climbing. The drive motor shall provide sufficient torque, and the elastic arms shall generate enough normal pressure to produce static friction and prevent slipping. According to theoretical calculations, the motor torque shall be no less than 0.2 N·m, and the spring stiffness shall be designed such that the wheel-wall normal pressure is at least twice the robot's weight.The robot shall move smoothly inside the pipeline at a controllable speed within 0.05–0.1 m/s to avoid image blur caused by speed fluctuations or vibration. The control system shall support precise speed regulation via PWM or FOC and be capable of differential steering. Meanwhile, the total weight shall be controlled within 500 g to avoid secondary damage to the pipeline.

3.5 Requirements for User Interaction and Result Presentation

Operators generally lack professional knowledge of computer vision, so the system must provide a simple and intuitive graphical user interface (GUI) that displays real-time RGB images, depth images, fused thermal bead annotation images inside the pipeline, and the mapped positions of thermal beads in the global pipeline trajectory. The volume ratio and graded alarm levels of thermal beads shall be distinguished by colors and supplemented with text prompts.Field inspections may be conducted using laptops or tablets with different operating systems, so the front-end of the system must be cross-platform compatible. It can be developed using the PyQt5 framework without relying on specific runtime environments.Upon completion of inspection, the system shall automatically generate a report containing thermal bead positions, volume ratios, grading conclusions, trajectory diagrams, and on-site images to facilitate archiving and construction decision-making. The report format shall comply with the specifications of engineering acceptance documents.

4. System Design

4.1 Overall Architecture Design

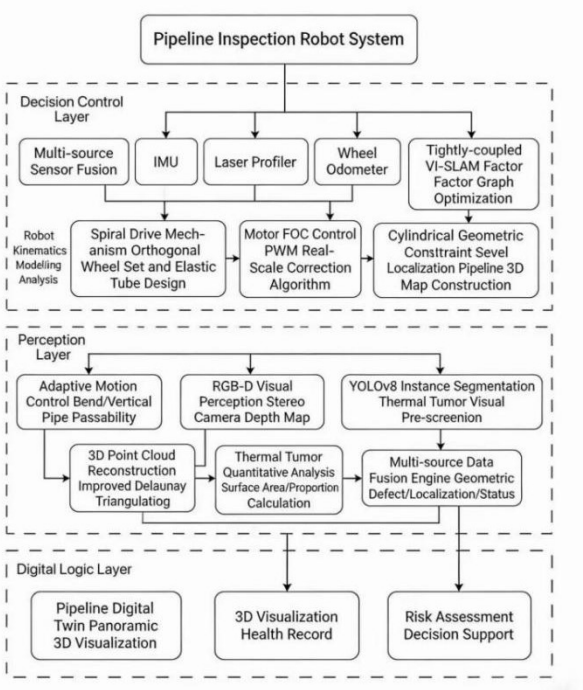

Figure 3. Overall system technical flowchart

ISSN: 2414-1895 DOI: 10.6919/ICJE.202604_12(4).0023

To realize the non-destructive detection, accurate quantification and spatial positioning of thermal beads inside pipelines, this system takes visual perception–precise positioning–intelligent control–digital mapping as the technical thread, and constructs a complete automatic detection system for internal pipeline defects.Centered on RGB-D vision and multi-sensor fusion, the system uses Raspberry Pi 4B as the core processing unit, which is responsible for running image recognition and positioning algorithms, as well as controlling the motion of the screw drive mechanism. Meanwhile, a host computer interactive interface is developed based on the PyQt5 framework, supporting real-time visualization of the detection process and report generation.This integrated architecture of edge computing + visualization terminal not only ensures the real-time performance of algorithm execution in the complex internal environment of pipelines, but also achieves convenient human-computer interaction, providing full-process data support for engineering quality evaluation and operation and maintenance management.

4.2 Functional Module Design

The hardware of this system is designed around the screw-driven wall-pressure-adaptive driving structure and the multi-sensor fusion perception unit, ensuring the robot achieves excellent passability and detection performance in narrow, curved non-metallic pipelines.

4.2.1 Mechanical Structure and Driving System

The robot adopts two sets of orthogonally distributed three-wheel driving units (as shown in Figure 4). The rear wheel set is installed obliquely at an inclination angle of 15°–18° to form a screw propulsion mode. The front wheel set is arranged along the pipeline axis to carry the detection sensors.

This structure combines the controllability of a wheeled system with the superior bend passability of screw driving. Stable adhesion to the pipe wall is achieved through elastic arms and high-friction rubber wheels.

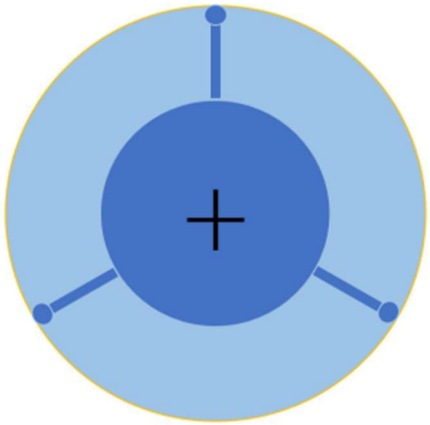

Figure 4. Structure of the orthogonal three-wheel mechanism

Based on kinematic analysis (as shown in Figure 5), the helical trajectory of the robot in a straight pipe can be described as follows:

$$r(t) = \begin{bmatrix} R\cos(\omega t) \\ R\sin(\omega t) \\ v_z t \end{bmatrix}$$

where$R$is the inner radius of the pipe,$\omega$is the angular velocity of the rotor, and$v_z$is the axial velocity.

ISSN: 2414-1895 DOI: 10.6919/ICJE.202604_12(4).0023

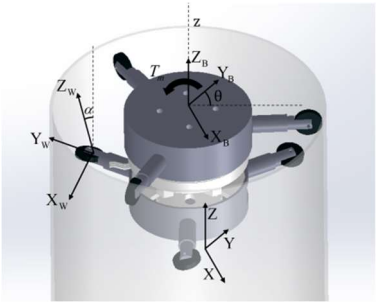

Figure 5. Kinematic analysis of the robot inside the pipeline

In a curved pipe environment, stable passage through a 90° bend with a curvature radius of not less than 150 mm can be achieved by adjusting the wheel inclination angle and motor torque (simulated trajectory shown in Figure 6).

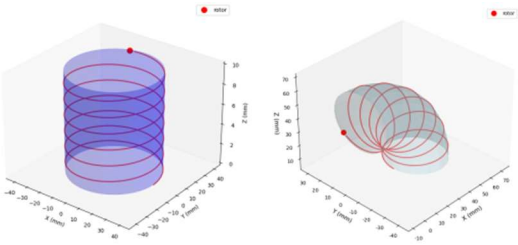

Figure 6. Trajectory of the rotor wheel moving along the z-axis in straight / curved pipes

4.2.2 Core Control and Perception Unit

The control system is centered on the Raspberry Pi 4B, which drives brushless motors via GPIO interfaces and PWM signals, and integrates a binocular camera and a 9-axis IMU. The binocular camera is used to acquire RGB images and depth maps, while the IMU provides real-time attitude and acceleration data. Both are fixed by a rigid bracket and calibrated for extrinsic parameters to ensure precise alignment between visual information and spatial position.After time synchronization of sensor data, the Raspberry Pi runs the RGB-D fusion algorithm based on the CBAM attention mechanism, as well as the YOLOv8-SAM object detection and segmentation model, to achieve pixel-level identification and 3D reconstruction of thermal beads. Meanwhile, complementary filtering and factor graph optimization are adopted to fuse IMU and visual information, enabling robot trajectory estimation and spatial annotation of thermal beads in GPS-denied environments.

To realize the automatic identification, 3D reconstruction and quantitative evaluation of hot-melt joint defects on the inner wall of pipelines, this system constructs an algorithm framework integrating computer vision, 3D point cloud processing and multi-sensor fusion positioning. Centered on YOLOv8 instance segmentation, improved Delaunay triangulation and VILL-SLAM tightly coupled optimization, this framework supports the accurate identification of thermal beads, precise calculation of surface area and spatial positioning of defects respectively, forming a complete algorithm closed-loop from image acquisition to quantitative evaluation.

4.3 Algorithm Support

4.3.1 Thermal Bead Recognition Algorithm based on YOLOv8 and Depth Information Fusion

The thermal nodule identification stage employs a dual-assurance strategy of “visual preliminary screening + depth-based refined filtering.”First, RGB images are input into the pre-trained YOLOv8-seg model to output the initial segmentation mask of thermal beads. Adopting an instance segmentation architecture, this model can efficiently extract pixel-level boundaries of thermal bead regions and adapt to complex illumination and texture variations inside the pipeline.

ISSN: 2414-1895 DOI: 10.6919/ICJE.202604_12(4).0023

To further suppress false detections, the system introduces depth information for refinement. Let the depth values of pixels within the initial mask region be

$D = \{d_1, d2, \ldots \ldots, d_n\}$,with a median value of d. The representative distance of the thermal bead is then defined as:

$$d_{rep} = \text{median}(D)$$

Set a dynamic depth tolerance range Δd (e.g., ±0.03 meters) centered at d_{rep} to generate the depth mask:

$$M_{depth}(u,v) = \begin{cases} 1, & |d(u,v) - d_{rep}| \le \Delta d \\ 2, & \text{otherwise} \end{cases}$$

The final thermal bead mask is fused by performing a logical AND operation on the visual mask and the depth mask:

$$M_{final} = M_{YOLO} \wedge M_{depth}$$

This dual verification mechanism effectively filters out false targets caused by light reflections or pipeline texture interference, significantly improving recognition accuracy.

4.3.2 Surface Area Calculation Algorithm based on Improved Delaunay Triangulation

After obtaining the refined thermal bead mask, the system achieves accurate quantification of the surface area through 3D point cloud reconstruction.First, the camera intrinsic matrix is used to back-project each pixel in the mask and its corresponding depth value into 3D space, generating an initial dense point cloud:

$$[X, Y, Z] = Z \cdot [\frac{u-c_x}{f_x}, \frac{u-c_y}{f_y}, 1]$$

where $f_x, f_y$are focal lengths, and, $c_x, c_y$are coordinates of the principal point.

In response to the curved surface characteristics of pipelines and noise interference, this system improves the classical Delaunay triangulation algorithm. A point cloud filtering mechanism based on normal vector consistency in local neighborhoods is introduced to remove discrete noise points. Meanwhile, the two-dimensional boundary of the refined mask is adopted as a geometric constraint to ensure the triangulation process is strictly confined within the effective region of the thermal bead.

Let the filtered point cloud set be $P = \{p_1, p_2, \ldots, p_m\}$, Boundary-constrained Delaunay triangulation is used to generate a triangular mesh $T = \{t_1, t_2, \ldots, t_k\}$, where each triangular face $t_j$is composed of three vertices. The surface area S of the thermal bead is calculated as follows:

$$S = \sum_{j=1}^{k} \frac{1}{2} \left\| (p_{j2} - p_{j1}) \times (p_{j3} - p_{j1}) \right\|$$

This algorithm achieves millimeter-precision measurement of the surface area of irregular thermal beads, overcoming perspective errors in two-dimensional image measurement.

ISSN: 2414-1895 DOI: 10.6919/ICJE.202604_12(4).0023

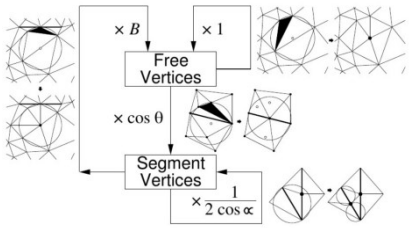

Figure 7. Improved principle of the triangulation algorithm

4.3.3 Factor Graph Optimization-Based Tightly Coupled SLAM Algorithm

To achieve precise spatial positioning of thermal beads inside pipelines, this system establishes a tightly coupled SLAM algorithm based on factor graph optimization, which fuses information from four types of sensors: vision, IMU, laser profiler, and LiDAR.

The system state vector is defined as:

$$\chi = [x_0, x_1, \ldots, x_n, \lambda_0, \lambda_1, \ldots, \lambda_m]$$

where $X_k = [T_{b_k}^w, v_{b_k}^w, b_a, b_g]$represents the pose, velocity, and sensor biases of the k-th keyframe.

The optimization framework integrates the following four constraint factors:

Visual reprojection factor: constrains the reprojection error of feature points across multiple frames;

IMU preintegration factor: provides high-frequency motion priors and enhances robustness when features are missing;

Vision-depth correlation factor: uses direct depth measurements from the laser profiler to constrain feature point depth estimation;

LiDAR factor: designed for pipeline geometric characteristics, including cylindrical constraints and ICP registration.

To address the scale ambiguity problem in pipeline environments, an active depth correction mechanism is introduced:$\bar{s} = \alpha \frac{1}{|F_l|} \sum_{f_i \in F_l} \frac{\bar{d_l}}{\hat{d_l}} \hat{s} + (1-\alpha) \frac{1}{|F_L|} \sum_{f_i \in F_L} \frac{\bar{d_l}}{\hat{d_l}} \hat{s}$

where$F_L$and $F_L$denote the feature point sets of the laser profiler and LiDAR respectively, and α is the balance weight. Experiments show that the average odometry drift of this algorithm in a 22-meter pipeline is reduced to 0.84%, which is a 6.6-fold improvement over the traditional VINS-Mono algorithm.

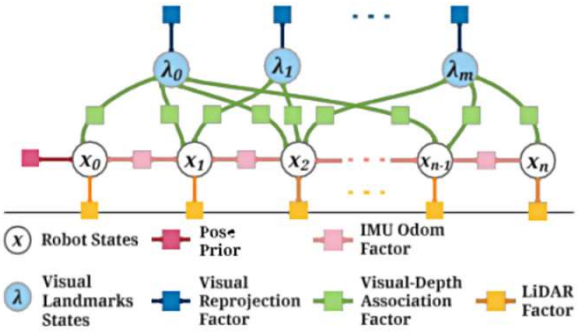

Figure 8. Factor graph optimization framework based on sliding window

4.3.4 Thermal Bead Proportion Threshold Judgment Model

To quantify the influence of thermal beads on the hydraulic performance of pipelines, the system constructs a thermal bead proportion judgment model based on fluid mechanics and engineering specifications.Let the original inner diameter of the pipeline be D , the volume of the thermal bead be

ISSN: 2414-1895 DOI: 10.6919/ICJE.202604_12(4).0023

V_{bead},and the volume of the pipeline per unit length be V_{pipe}. The thermal bead volume ratio η is defined as:

$$\eta = \frac{V_{bead}}{V_{pipe}} \times 100\%$$

According to the incompressible fluid continuity equation $Q = Av$, thermal beads reduce the effective cross-sectional area A, causing an increase in flow velocity v and local pressure drop.

Combined with the Code for Construction and Acceptance of Water Supply and Drainage Pipeline Engineering and practical engineering experience, the thermal bead proportion is divided into three levels:

$\eta < 5\%$: Safe state, no intervention required;

$5\% \leq \eta \leq 10\%$: Acceptable state, marking and observation recommended;

$\eta > 10\%$: Unacceptable state, cutting and replacement recommended.

This model provides a quantitative basis for automatic system early warning and engineering decision-making.

4.4 3D Reconstruction and Visualization Implementation

Based on the optimized pose data, the system generates an accurate environmental model through a parallel mapping process. Laser scanning produces a dense colored point cloud map, where each laser point is colored using adjacent visual frames to form realistic 3D reconstruction results.Meanwhile, LiDAR point clouds are downsampled via voxel grid filtering to construct a lightweight local map, maintaining bounded memory usage while preserving positioning accuracy.

To comprehensively improve system practicability, a dedicated visualization platform is developed based on Matplotlib, with output effects shown in the figure:

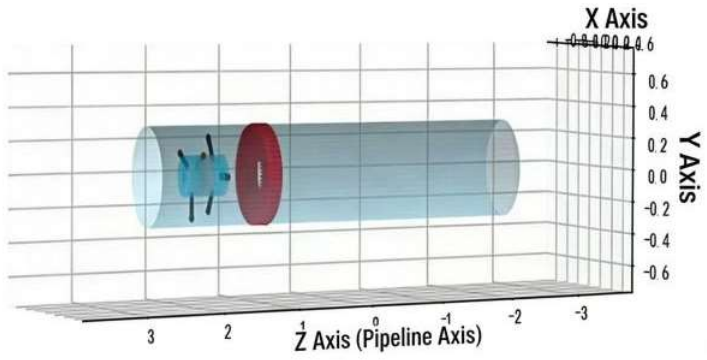

Figure 9. 3D pipeline simulation and thermal bead positioning visualization

The interface displays the robot's helical motion trajectory and the 3D pipeline reconstruction process in real time, distinguishing normal pipe regions from thermal bead defect areas using a unique coloring scheme.The "3D health archive" established by the system not only provides a basis for reviewing and verifying thermal bead identification results, but also supports complete data for remote collaboration, staff training, and responsibility tracing.In practical scenarios such as the renovation of old residential communities, this non-invasive and accurate detection method significantly improves the efficiency and reliability of pipeline maintenance.

ISSN: 2414-1895 DOI: 10.6919/ICJE.202604_12(4).0023

5. Experimental Validation

5.1 Experimental Design

To comprehensively verify the effectiveness and robustness of this system, experiments were conducted in a simulated PPR pipeline environment set up in the Embedded Systems and Internet of Things Application Laboratory at North China University of Science and Technology. The experimental pipeline network includes typical structures such as horizontal straight pipes (1.5m), vertical straight pipes (1.2m), 90° elbows (radius of curvature 150mm), and T-shaped tees, with a total length of approximately 4.2 meters and an inner diameter of Φ32mm, to simulate the complex working conditions of real building water supply networks. Ten artificially prefabricated thermal bead defect points were selected for the experiment, with their volume proportion ranging across three levels: safe (<5%), acceptable (5%-10%), and unacceptable (>10%). The experimental comparison benchmark is the traditional manual visual inspection combined with endoscope-assisted detection methods, comprehensively evaluating the system's performance from three aspects: detection efficiency, quantitative accuracy, and passability.

5.2 Efficiency and Passability Validation

By comparing the time consumption and success rate of completing a full-process task (from entrance to exit and generating a report) between manual inspection and the automated detection of this robot, the system's advantages are quantified. The experimental results are shown in Table 2.

Table 2. Comparison of Detection Efficiency and Passability

Task Indicator	Manual Inspection	This System	Efficiency Improvement
Average full-process time	42 minutes	8 minutes	5.25 times
Complex bend (90° + T-type) pass success rate	60% (3/5 times)	100% (5/5 times)	+40 percentage points
Preliminary localization time of thermal beads	15-25 minutes	<1 minute	40 times
Total	6.5 hours	2 minutes 15 seconds	390 times

Conclusion: As shown in Table 1 (Note: referring to the table data discussed), this system not only shortens the single detection time from over 40 minutes to under 8 minutes, but more importantly, its unique screw-driven structure ensures 100% reliable passability in pipelines containing vertical sections and complex elbows, completely solving the problem of traditional methods being difficult to penetrate or getting stuck in non-straight pipelines.

5.3 Quantitative Accuracy Comparison

To verify the accuracy of the system's thermal bead volume quantification algorithm, the measurement results of this system were compared with the real volume of the thermal beads (Ground Truth) obtained by a high-precision laser scanner. Five thermal bead samples with different volume proportions were randomly selected for testing in the experiment.

Experimental Results:

Manual Inspection: Can only make qualitative judgments (presence/absence) or rough grading, and cannot provide any quantitative data.

This System's Analysis: The average relative error is 4.7%.

ISSN: 2414-1895 DOI: 10.6919/ICJE.202604_12(4).0023

Error Analysis: The main sources of error are local noise in the depth map caused by reflections on the inner wall of the pipeline, and the segmentation uncertainty in the transition area between the thermal bead edge and the pipe wall. By optimizing the CBAM attention weight and post-processing filtering, this error has been controlled within an engineering-acceptable range (<5%), which is sufficient to support the graded alarm threshold determination of 5%-10%.

5.4 Functional Display and User Evaluation

The system integrates a complete hardware and software interactive platform, mainly including two core functional modules: real-time detection and 3D visualization; the interface effect is shown in Figure 10.

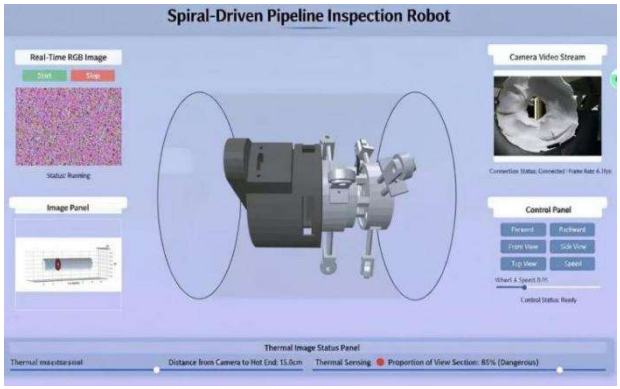

Figure 10. Human-computer interaction control interface of the pipeline inspection robot

Operators can monitor the running status of the robot in real-time through the interface. The left side of the interface synchronously displays the RGB image, depth map, and the fused RGB-D feature map; the right side dynamically draws the robot's motion trajectory calculated based on the IMU, and accurately marks the positions of the identified thermal beads on the trajectory.

When the robot detects a thermal bead, the system can instantly generate a 3D point cloud model of the defect point and calculate its volume and volume ratio per unit length of the pipeline. The bottom of the interface will automatically provide engineering treatment suggestions such as "Safe", "Observation Recommended", or "Cutting and Replacement Recommended" based on preset thresholds.

6. Conclusion

The screw-driven pipeline inspection robot system based on the RGB-D recognition and quantification algorithm developed in this study aims to solve the problem of non-destructive testing for thermal bead defects in PPR pipelines. By integrating the CBAM attention mechanism, RGB-D multimodal perception, IMU inertial navigation, and the screw drive structure, it effectively overcomes the core pain points of traditional manual inspection-"low efficiency, poor accuracy, high cost, and unquantifiable"-achieving high-precision recognition, 3D volume reconstruction, and precise spatial positioning of thermal beads. Its core value lies in building a closed-loop intelligent detection framework oriented towards non-metallic small-diameter pipelines, which not only supports engineers in quickly locating defect positions and making scientific maintenance decisions based on quantitative thresholds (5%, 10%), but also provides an implementable technical path for the active health management of building water supply and drainage systems. On a technical level, the collaborative design of the Raspberry Pi embedded platform and the PyQt5 cross-platform interface verifies the practicability and deployability of this system in real engineering scenarios, and its modular hardware and software architecture also reserves flexible expansion space for subsequent adaptation to different pipe diameters or defect types. Future research could further introduce federated learning or online adaptive calibration mechanisms to enhance the model's generalization

ISSN: 2414-1895 DOI: 10.6919/ICJE.202604_12(4).0023

ability under complex lighting and material changes, and explore multi-robot collaborative operation modes to support efficient general surveys of large-scale pipeline networks, thereby driving the evolution of pipeline inspection from single-point fault response to a comprehensive intelligent operation and maintenance ecosystem.

References

[1] Bandala A A, Maningo J M Z, Jose J A C, et al. Development of an adaptive pipeline inspection robot with rust detection capability [C]. 2018 IEEE Region Ten Symposium (Tensymp), 2018: 271-276.

[2] Roh S, Choi H R. Differential-drive robots for city gas pipelines [J]. IEEE Transactions on Robotics, 2005, 21(1): 1-17.

[3] Kahnamouei J T, Moallem M. A review on pipeline robots [J]. Ocean Engineering, 2023, 277: 114260.

[4] Han Weitao, Wen Tao, Liu Lei, et al. Design of soft pipeline robot based on Kresling origami structure [J]. Journal of Engineering Design, 2025, 32(01): 72-81.

[5] Bradski G, Kaehler A. Learning OpenCV: Computer Vision with the OpenCV Library [M]. O'Reilly Media, 2008.

[6] Woodman O J. An introduction to inertial navigation [R]. University of Cambridge, Computer Laboratory, 2007.

[7] Kahnamouei J T, Moallem M. A review on pipeline robots [J]. Ocean Engineering, 2023, 277: 114260.

[8] Tian T, Wang L, Yan X, et al. VILL-SLAM: Real-time dense RGB-D mapping for pipeline environments [C]. 2023 IEEE/RSJ International Conference on Intelligent Robots and Systems (IROS), 2023: 1525-1531.